Models of AC and DC cable systems for technical and economic evaluation of offshore wind farm connection

Swann Gasnier
SuperGrid Institute, Villeurbanne, France.
Email: swann.gasnier@supergrid-institute.com

Aymeric André, Serge Poullain
SuperGrid Institute, Villeurbanne, France.
Email: {aymeric.andre, serge.poullain }@supergrid-institute.com

Vincent Debusschere
G2ELab, Grenoble, France.
Email: vincent.DEBUSSCHERE@g2elab.grenoble-inp.fr

Bruno Francois
L2EP, Villeneuve d'Ascq, France.
Email: bruno.francois@centralelille.fr

Philipe Egrot
EDF Lab Renardières, France.
Email: philippe.egrot@edf.fr

Abstract— **Accurate cable modeling is a recurrent issue for electric architecture evaluation and design, especially in specific contexts, like offshore wind farms.**
This paper proposes optimal analytical cable models for the technical and economic assessment of offshore wind generation systems.
Proposed models evaluate the electrical and thermal behaviors of cables, as components of the complete offshore wind generation transmission system. The cost effectiveness of the latter is assessed by considering both CAPEX and OPEX contributions.
A comparison with published models is also presented, and illustrated on various cable designs. Among others, we can see that the greater the section, the more interesting the simplification model is. Also, we checked that the model proposed by Brakelmann is correct in DC. For all other cases, the model, based on standards, is preferred.
The proposed paper goes beyond cables modeling by describing an assessment method based on specific cables modeling, allowing the choice of cables within a holistic assessment tool bringing decision support regarding optimal design of offshore wind farm grid connection.
A system assessment based on the proposed model is presented, for a typical HVAC architecture.

Index Terms— **Cables, CAPEX, electrical behavior, HVAC, HVDC, IEC 60287, modeling, offshore wind farms, OPEX, thermal behavior.**

I. Acronyms

PARAMETERS FOR GEOMETRICAL PROPERTIES

Symbol	Quantity	Unit [a]
D'_a	External diameter of the armor	m
D_e	External diameter of one cable	m
D_i	External diameter of insulation	m
N_w	Number of steel wires of the armor	
d_A	Internal diameter of the armor	m
d_c	Diameter of one core	m
s_1	Distance between cables axes	m
t_1	Thickness of the insulation including semi-conductive layers	m
t_3	Thickness of the outer covering	m
t_{PE}^s	Thickness of the « inner plastic sheath »	m
t_b	Thickness of the bedding itself	m
t_s	Thickness of the metallic sheath	m
δ_A	Diameter of one steel wire of the amour	m
L	Burying depth of cables	m
c	Distance between the axis of a conductor and the cable center (only for three-core cables)	m
s	Axial distance between core conductors	m

PARAMETERS FOR ELECTRIC PROPERTIES

Symbol	Quantity	Unit [a]
R_0	DC resistance of the conductor at 20°C	Ω/m
$R_A^{\theta_A}$	Per unit length resistance of the armor at temperature θ_A	Ω/m
R_{AC}^{θ}	AC resistance for a given conductor temperature θ	Ω/m
R_{DC}^{θ}	DC resistance of the conductor at maximum operating temperature	Ω/m
$R_S^{\theta_S}$	Per unit length resistance of the metallic sheath at temperature θ_S	Ω/m
w_d	Dielectric losses in the insulation	W/m
α_{20}^A	Armor temperature coefficient of electrical resistivity at 20 °C	K^{-1}

α_{20}^{c}	Conductor temperature rise coefficient of electrical resistivity at 20 °C	K^{-1}
α_{20}^{s}	Metallic sheath temperature coefficient of electrical resistivity at 20 °C	K^{-1}
α_T	Factor for conductor resistivity rise	
ε_r	Relative permittivity of insulation	
λ_1'	Factor taking into account the screening effect of the sheath	
λ_{sheath}	Sheath losses factor	
ρ_A	Resistivity of the armor at 20°C	Ω.m
ρ_s	Resistivity of the metallic sheath at 20°C	Ω.m
U_0	Phase to ground (core to metallic sheath) RMS voltage	V
C	Core to ground equivalent capacitance	F/m
I	RMS current in one core conductor	A
X	Per metallic sheath equivalent reactance	Ω/m
l	Inductance per core conductor	H/m
$tan\delta$	Loss angle of the insulating material	

PARAMETERS FOR THERMAL PROPERTIES

Symbol	Quantity	Unit [a]
θ	Operating temperature of the conductor	°C
θ_A	Temperature of the armor	°C
θ_S	Temperature of the metallic sheath	°C
θ_u	External temperature	°C
T_1	Per unit length thermal resistance of the layer(s) between the core conductor and the metallic sheath	K.m/W
T_2	Per unit length thermal resistance of the layer(s) between the metallic sheath and the armor	K.m/W
T_3	Per unit length thermal resistance of the outer layer of the cable	K.m/W
T_4	Per unit length thermal resistance of the sea bed at the proximity of the cable	K.m/W
ρ_T^s	Soil thermal resistivity	K.m/W
ρ_t^b	Thermal resistivity of the cable bedding	K.m/W
ρ_t^i	Thermal resistivity of the insulation	K.m/W
ρ_t^{oc}	Thermal resistivity of the outer covering	K.m/W

II. INTRODUCTION

Offshore wind applications offer a lot of scientific challenges. One of them consists of being able to design, optimize or just assess the economic viability of possible infrastructures used to connect offshore wind farms to shore. Depending on the considered system, HVAC but also HVDC cables need to be modeled (cabling system is the main driver in favor of DC). The savings in losses and CAPEX obtained in regard to cables can overcome the additional costs associated to additional systems required for the DC technology to operate (converter station and associated platform if located offshore).

Cables represent then a key component in the assessment of the complete system connecting offshore wind farms to shore and most of the studies are based on a very limited number of analytical models for losses evaluation.

Lazaridis, Ackermann and al. [1] (2005) and Lundberg [2] (2009) are pioneers in the assessment and comparison of network architectures connecting offshore wind farms to shore. More recently, some studies were focused on the assessment [3–5] or optimization [6–8] of industrially deployed collection and transmission technologies. Others assess innovative proposals [9–11]. Finally, some of the assessment studies are done with an emphasis on the HVAC cabling system [12–15].

We can cite three main sources for cable modeling, which are IEC 60287 standards [16], [17], a model proposed by H. Brakelmann [18] and a simplification, considering a constant maximal temperature in the cable.

In this paper, we discuss the validity of those models, propose the complete explicit analytic model from IEC 60287 standards, and illustrate and compare those models on typical cables for various sections and voltages. Finally, we illustrate the usage of such models in a system level perspective, by evaluating the capitalized cost due to losses for a given architecture based on cables modeling.

III. CABLES MODELS BASED ON STANDARD IEC 60287

The objective of the IEC 60287 standard is to compute the ampacity of a cable. The ampacity is the current which does not induce a temperature in the conductor higher than the maximal acceptable value for the insulation capability (for example 90°C for XLPE AC cables and 70°C for XLPE DC cables) [19]. For that purpose, models are proposed in that standard to compute losses of an extensive set of cables and laying conditions. The models presented in this paper are extracted from this standard. Our objective is to propose a comprehensive set of models with all needed information for fast and accurate modeling of HVAC and HVDC connections for infrastructures assessment.

For that purpose, section A presents losses computation, section B is dedicated thermal resistances computation and in section C these models are coupled by using a power flow based on IEC 60287-2. Finally, section D illustrates the pertinence of those models on representative study cases.

A. Electric models for losses computation

The equations of this section are based on the standard IEC 60287-1 [16]. For AC cables, they have been previously proposed in [20] and [21]. The assumption of any drying-out of the soil has been made for the whole study, which is typically relevant for offshore applications

1) DC cables

An electric DC cable as presented in Fig. 1 presents no skin and proximity effects.

The model only consists in calculating the DC resistance R_{DC}^{θ} corresponding to the core conductor temperature θ expressed in (1).

$$R_{DC}^{\theta} = R_0.(1 + \alpha_{20}^{c}(\theta - 20)) \quad (1)$$

In this equation, the DC resistance of the conductor at 20°C is standardized and depends on the cross section (see Table 2 of [22]).

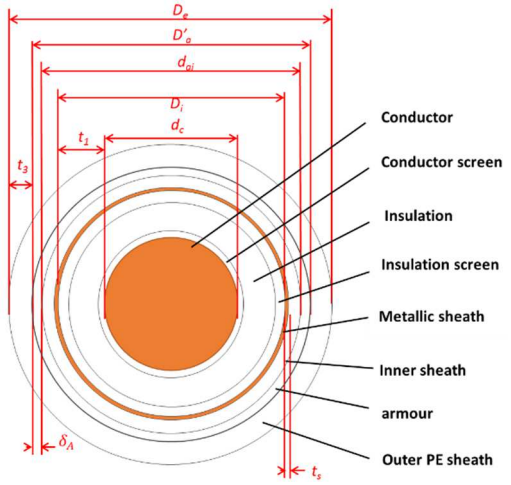

Figure. 1. Geometric parameters of DC cables.

2) AC cables

Unlike for DC cables, dielectric and induction losses must be considered for AC cables. Fig. 2 shows the required parameters of the model.

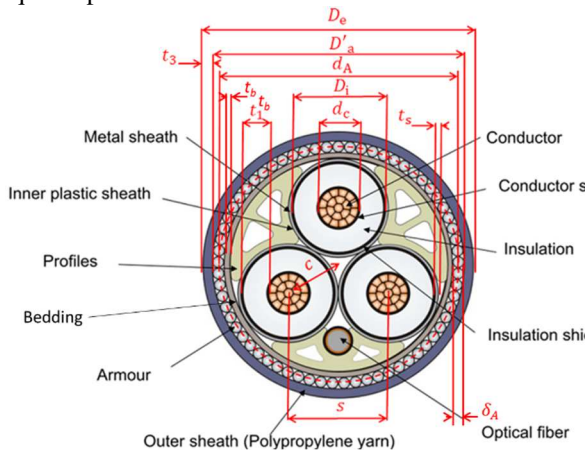

Figure. 2. Geometric parameters of AC cables.

For that purpose, per unit length inductances and capacitances are needed. They are usually extracted from datasheets [23], [19] or calculated directly by using (2) and (3).

$$C = \frac{\varepsilon_r}{18.\ln\left(\frac{D_i}{d_c}\right)}.10^{-9} \quad (2)$$

$$l = 2.10^{-7}.\left(\ln\left(\frac{2s}{d_c}\right) + 0.25\right) \quad (3)$$

a) AC conductor resistance

The model of the AC cable is based on the model of the DC cable. The first step is to compute the AC resistance which takes into account proximity and skin effects, expressed in (4), (5) and (6).

$$R_{AC}^{\theta} = R_{DC}^{\theta}.\left(1 + y_s + y_p\right) \quad (4)$$

$$y_s = \frac{x_s^4}{192 + 0.8x_s^4} \quad (5)$$

$$y_p = \frac{x_p^4}{192 + 0.8x_p^4}\left(\frac{d_c}{s}\right)^2.\left(0.312\left(\frac{d_c}{s}\right)^2 + \frac{1{,}18}{\frac{x_p^4}{192 + 0.8x_p^4} + 0.27}\right) \quad (6)$$

With x_s and x_p being arguments of a Bessel function used to calculate skin effect; it can be obtained with (7) and (8).

$$x_s^2 = \frac{8\pi f}{R_{DC}^{\theta}}.10^{-7}.k_s \quad (7)$$

$$x_p^2 = \frac{8\pi f}{R_{DC}^{\theta}}.10^{-7}.k_p \quad (8)$$

Where k_s and k_p depend on the geometry of the conductor and are given in Table 2 of the standard IEC 60287-1. For example, for non-impregnated copper round stranded conductor, $k_s = 1$ and $k_p = 1$.

b) Losses in metallic sheath

The IEC 60287 standard specifies how to calculate the losses in the metallic sheath by using the "sheath losses factor" λ_{sheath} which is the ratio between the losses in one metallic sheath and the losses in the associated core conductor.

$$\lambda_{sheath} = \lambda_{sheath}^{cir} + \lambda_{sheath}^{eddy} \quad (9)$$

Where:

λ_{sheath}^{cir} is the part of λ_{sheath} caused by circulating current in the sheath, expressed in (10).

λ_{sheath}^{eddy} is the part of λ_{sheath} caused by circulating eddy currents in the sheath. For a three core cable such as the one considered here, with a metallic sheath per core conductor, there are no losses relative to eddy current, thus $\lambda_{sheath}^{eddy} = 0$

$$\lambda_{sheath}^{cir} = \left(\frac{R_S^{\theta s}}{R_{AC}^{\theta}}\right).\frac{1.5}{1 + \left(\frac{R_S^{\theta s}}{X}\right)^2} \quad (10)$$

Where X is given in (11) and $R_S^{\theta s}$ is calculated in (12).

$$X = 4\pi f.10^{-7}.\ln\left(\frac{2s}{D_i + t_s}\right) \quad (11)$$

$$R_S^{\theta s} = \frac{\rho_s}{\pi((D_i + t_s)^2 - D_i^2)}.\left(1 + \alpha_{20}^s(\theta_S - 20)\right) \quad (12)$$

Where:

$(D_i + t_s)$ corresponds to the "mean diameter of the screen", as defined in the standard 60287-1, expressed in meters.

$\pi((D_i + t_s)^2 - D_i^2)$ corresponds to the cross section of the metallic sheath, expressed in square meters.

c) Losses in the armor

The IEC 60287 standard specifies how to calculate the losses in the armor sheath by using the "armor losses factor" λ_{armor}. It is the ratio between the third of the losses in the armor and the losses in one core conductor.

$$\lambda_{armor} = 1{,}23\frac{R_A^{\theta_A}}{R_S^{\theta_S}}\left(\frac{2c}{d_A}\right)^2 . \frac{1 - \frac{R}{R_S^{\theta_S}}\lambda_1'}{\left(\frac{2.77R_A^{\theta_A}10^6}{2\pi f}\right)^2 + 1} \quad (13)$$

Where $R_A^{\theta_A}$ is given in (14) and λ_1' in (15).

$$R_A^{\theta_A} = \frac{4.\rho_A}{N_w.\pi.\delta_A^2}.\left(1 + \alpha_{20}^A(\theta_A - 20)\right) \quad (14)$$

$$\lambda_1' = \left(\frac{R_S^{\theta_S}}{R_{AC}^{\theta}}\right).\frac{1}{1 + \left(\frac{R_S^{\theta_S}}{X}\right)^2} \quad (15)$$

Cable manufacturers introduce an empirical formula to take into account skin effects in armors to calculate their losses per unit of length resistance. It is commonly acknowledged by the cable community that losses in three-core armored cables are overestimated when they are calculated according to IEC-60287 [24], [25].

d) Dielectric losses in the insulation

The dielectric losses in the insulation w_d depends on the voltage. The dielectric loss per unit length in each phase is given in (16), where C is calculated by using (2).

$$w_d = 2\pi f.C.U_0^2.tan\delta \quad (16)$$

For load flows computations, the resistance will be considered as an equivalent AC resistance which takes into account the losses in the metallic sheaths and in the armor.

$$R_{AC,eq} = R_{AC}^{\theta}(1 + \lambda_{sheath} + \lambda_{armour}) \quad (17)$$

B. Thermal model

The thermal model proposed in the IEC standard 60287-2 is based on the calculation of thermal resistances [17]. It is therefore assumed that the thermal steady state is reached, which can be a restrictive hypothesis. No thermal dynamics are modeled, thus, the resulting quantifications of losses and ampacity are conservative.

In the standard, four different resistances are calculated, between the core conductor, the metallic sheath, the armor, the outer layer of the cable and the sea bed at the vicinity of the cable, noted T_1 to T_4.

T_1 and T_3 formally do not depend on whether the cable is for AC or DC currents. T_1 is proposed in (18) and T_3 in (19).

$$T_1 = \frac{\rho_t^i}{2\pi}.\ln\left(1 + \frac{2t_1}{d_c}\right) \quad (18)$$

$$T_3 = \frac{\rho_t^{oc}}{2\pi}.\ln\left(1 + \frac{2t_3}{D_a'}\right) \quad (19)$$

1) Specific thermal resistances for DC cables

For a DC cable, two specific thermal resistances are considered. The first one, T_2, is expressed by (20).

$$T_2 = \frac{\rho_t^b}{2\pi}.\ln\left(\frac{d_{ai}}{D_i + 2t_s}\right) \quad (20)$$

The second one, the thermal resistivity of surrounding soil, T_4, depends on the laying conditions. For existing DC power cables, there are normally two cables, with opposite polarities and with currents in opposite directions. They are buried in trenches, either in a common trench, or in two different ones. Another well spread technology is bundled cables. Depending on that, mutual heating will significantly influence ampacity and losses. For a DC cable, T_4 is then defined by considering a mutual heating. In (21) the expression of T_4 is given for "two cables having equal losses, laid in a horizontal plane, spaced apart".

$$T_4 = \frac{1}{2\pi}\rho_T^s.\left(\ln\left(u + \sqrt{u^2 - 1}\right) + \frac{1}{2}\ln\left(1 + \left(\frac{2L}{s_1}\right)^2\right)\right) \quad (21)$$

Where u is given in (22).

$$u = \frac{2L}{D_e} \quad (22)$$

In practice, L and s_1 (parameters defining laying conditions) have a significant impact on T_4. L is usually standard (typically in the range of 1-2m to obtain a protection from all external damages such as anchors) but s_1 depends on installation choices. For example, if one trench is considered (because less costly), the worst case should be considered, where $s_1 = D_e$.

2) Specific thermal resistances for AC cables

For AC cables, T_2 is expressed in (23).

$$T_2 = \frac{1}{6\pi}\rho_t^b.G \quad (23)$$

Where: G is a factor obtained by using an empirical curve provided in the IEC 60297-2 standard. The value is obtained calculating the rate r_G proposed in (24) and by using the bottom curve of [17] to get the corresponding factor. The curve can be implemented in the model of the cable as a look up table.

$$r_G = \frac{t_b + t_{PE}^s}{D_i + 2t_s} \quad (24)$$

For an AC cable, T_4 is given in (25), with u given in

(22).

$$T_4 = \frac{1}{2\pi}\rho_T^S.\ln\left(u+\sqrt{u^2-1}\right) \quad (25)$$

C. Thermo-electric models coupling for more accurate losses and ampacity evaluation

For a DC cable, the power balance between a conductor and its environment gives (26), where $\Delta\theta$ is the difference between the temperature of the core conductor and the undisturbed temperature of the sea bed.

$$\Delta\theta = R_{DC}^{\theta}.I^2[T_1+T_2+T_3+T_4] \quad (26)$$

Where I is the rms current in one core conductor.
The phenomenon is more complex for AC than for DC cables.

For an AC cable, the power balance in steady state between the core conductor and the metallic sheath gives (27).

$$\theta_S = \theta - \left(R_{AC}^{\theta}.I^2 + 0.5.w_s\right).T_1 \quad (27)$$

The power balance in steady state between the core conductor and the armor gives (28). Where n=3 for three core AC cables.

$$\theta_A = \theta - \left(\left(R_{AC}^{\theta}I^2 + 0.5.w_s\right).T_1 + \left(R_{AC}^{\theta}I^2(1+\lambda_{sheath}) + w_d\right).n.T_2\right) \quad (28)$$

For an AC cable, the power balance between the conductor and the sea bed gives the difference between the temperature of the core conductor and the external temperature of the sea bed in (29).

$$\Delta\theta = I^2.\left(R_{AC}^{\theta}T_1 + nR_{AC}^{\theta}(1+\lambda_{sheath})T_2 + n.R_{AC}^{\theta}(1+\lambda_{sheath}+\lambda_{armour})*(T_3+T_4)\right) + W_d * \left(\frac{1}{2}.T_1 + n(T_2+T_3+T_4)\right) \quad (29)$$

The link between thermal and electrical models is done in the same way for DC and AC cables (even if it is slightly more complex for AC cables, which is the reason why only the AC case is proposed here). The ampacity of an AC cable can be calculated by using the algorithm whose synoptic is depicted on Fig. 5. The core conductor temperature of an AC cable θ corresponding to a current I and a resistance R_{AC}^{θ} can be calculated by using algorithms described in a very similar synoptic as the one proposed in Fig. 3.

The losses factors for the metallic sheath and the armor corresponding to this current I are also obtained in the process. The equivalent resistance that takes into account all currents-dependent losses in the cable $R_{AC,eq}$ can be calculated by using (17).

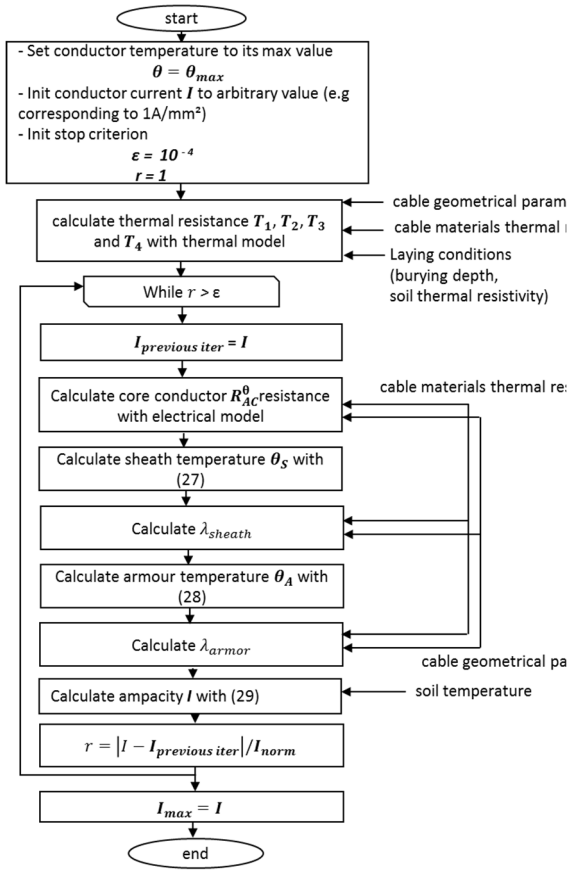

Figure.3. Algorithm flow chart for calculating the ampacity of an AC cable.

IV. Validation of the Models

A. DC cable model

Implemented models are validated on the basis of ampacity results because models are based on losses models and because the ampacity is the major parameter on which is based the variable model parameter (core resistance) of cables.

Results of calculated cable ampacity are given in TABLE I, that can be compared with ABB cables ampacities (with

$\theta_u = 15°C, \rho_T^S = 1K.W/m, L = 1m$)

TABLE I
VALIDATION OF DC MODEL ON THE BASIS OF AMPACITY

Section(mm²)	Ampacity from ABB (A) [19]	Ampacity from model at 320 kV (A)	Error (%)
1200	1458	1415	2.9 %
1500	1644	1595	3.0 %
1800	1830	1770	3.3 %
2000	1953	1889	3.3 %

Errors can be explained by approximate values used for the thickness of different layers and by interpretation of what corresponds to “close laying”. Besides, the same ampacity is given by ABB for all voltages, which, of course, is an approximation. In any case, obtained

results are close to data provided by manufacturers. Corresponding losses can be found very close to actual losses.

B. AC cable model

As public field measurements are very difficult to get, IEC 60287 standards is considered to be the reference. Ampacities and losses calculated according to standards are provided in Nexans public catalogue for 33kV submarine cables [21] (used for 630 mm²) and in non-public sheets from Nexans (used for 185 mm² and 300 mm²). These data serve as validation references for implemented models. Results are presented in TABLE II

TABLE II
VALIDATION OF AC MODEL ON THE BASIS OF AMPACITY

Section (mm²)	Soil thermal resistivity (W.K/m)	Burying depth (m)	Water temperature (°C)	Ampacity, Nexans data (A)	Ampacity, model (A)	Error (%)
185	1.0	1.0	32	390	394	1.0 %
300	0.7	0.3	25	670	674	0.6 %
630	1.0	1.0	20	721	715	0.8 %

Once again, obtained results are very close to manufacturers data, with errors being below 1%. Corresponding losses can be found very close to actual losses as well.

V. APPLICATIONS OF THE MODELS

A. Comparison with state of art scientific literature

1) Model proposed by H. Brakelmann

A mathematical development allowing not to use the iterative algorithm proposed in Section II was proposed by H. Brakelmann to calculate losses [18]. The main assumptions are similar to the standard, in particular, a thermal steady state is considered to be always reached, making possible the use of thermal resistances only. Thus, the conductor's resistances will depend on their operating temperature.

The calculation of the conductor's temperatures each time for all currents would make the computation process quite heavy. Therefore, a model was provided to directly take into account currents as input parameters to quantify resistances.

To do so, H. Brakelmann defines equivalent thermal resistance of cables T_{Ers} in (30) by taking into account all layers and even heating in different layers due to losses.

$$T_{Ers} = T_1 + n(1 + \lambda_{sheath}).T_2 + n(1 + \lambda_{sheath} + \lambda_{armor})(T_3 + T_4) \quad (30)$$

The temperature rises in conductors with the external temperature $\Delta\theta_L$ as reference for any current I, using T_{Ers}, as expressed in (31) and (32).

$$\Delta\theta_L = T_{Ers}.R_{AC}^{\theta}(\alpha_T.\Delta\theta_L + c_\alpha)I^2 \quad (31)$$

$$c_\alpha = 1 - \alpha_T(20°C - \theta_u) \quad (32)$$

Even if not expressed in [18], it should be noted that, when writing equation (31), several errors are introduced:

1. Proximity and skin effects factors depend on the actual DC resistance of the conductor and thus on its temperature.
2. The influence of dielectric losses on the temperature is neglected.

By using equation (31), for $I = I_{max}$ and assuming that T_{Ers} is constant, equal to its value for the maximal current, it appears that $\Delta\theta_L$ is only depending on constant parameters and the current I, as expressed in equation (33) and (34)..

$$\Delta\theta_L = \Delta\theta_{Lmax}.\frac{c_\alpha\left(\frac{I}{I_{max}}\right)^2}{c_m - \Delta\theta_{Lmax}.\alpha_T\left(\frac{I}{I_{max}}\right)^2} \quad (33)$$

$$C_m = 1 + \alpha_T(\Delta\theta_{Lmax} + \theta_u - 20°C) \quad (34)$$

Note that, in reality, λ_{sheath} and λ_{armor} are not constant and thus T_{Ers} either, which is not considered in this text.

Finally, the ratio between losses for any current I and maximal losses for I_{max} (respectively $P_{losses,I}$ and $P_{losses,Imax}$, without dielectric losses w_d) can be written by taking into account the increase in resistivity due to the temperature, as written in (35). Thus, by making the assumption that the term $\lambda_{sheath} + \lambda_{armor}$ is constant and that skin and proximity effects factor are also constant (these assumptions are not clearly expressed in [18]), by replacing $\Delta\theta_L$ with (33) in (35), (36) can be obtained, with ν_θ expressed in (37).

$$\frac{P_{losses,I}}{P_{losses,Imax}} = \frac{1 + \alpha_T(\Delta\theta_L + \theta_u - 20°C)}{1 + \alpha_T(\Delta\theta_{Lmax} + \theta_u - 20°C)}\left(\frac{I}{I_{max}}\right)^2 * \left(\frac{1 + \lambda_{sheath} + \lambda_{armor}}{1 + \lambda_{sheath,max} + \lambda_{armor,max}}\right) \quad (35)$$

$$P_{losses,I} = P_{losses,Imax}\left(\frac{I}{I_{max}}\right)^2.\nu_\theta + w_d \quad (36)$$

$$\nu_\theta = \frac{c_\alpha}{c_\alpha + \alpha_T.\Delta\theta_{Lmax}.\left[1 - \left(\frac{I}{I_{max}}\right)^2\right]} \quad (37)$$

Finally, ν_θ can be used to calculate the parametric resistance of conductors at the temperature θ_L, $R_{AC}^{\theta_L}$, with (38).

$$R_{AC}^{\theta} = R_{AC}^{\theta_{max}}.\nu_\theta \quad (38)$$

These analytical developments proposed by H. Brakelmann allow decoupling the calculation of voltage and current distributions from the calculation of losses. The former is done by using lines equations with the non-corrected resistance. The losses along the transmission cable are then calculated by using (36) and

(37) to compute the corrected resistance.

2) Quantitative validation, electric resistances

By assuming that implemented models coming from IEC 60287 standards are valid for AC and DC, losses are calculated for different loads. It is done for AC cables, on the one hand, with complete calculation by iteratively quantifying temperature of the conductor and on the other hand, by using the analytical factor ν_θ for each loading current, having calculated once the ampacity of the cable. The calculations are done with the following laying conditions: $\theta_u = 20°C$, $\rho_T^s = 1K.W/m$, and $L = 1m$. It will be the case for the paper left.

A "real" interpolated ν_θ set could then be built and used in AC cables models as it would use an analytical version of ν_θ. For DC cables, the analytical ν_θ can be used directly without errors.

With the assumptions formulated in [18], the skin and proximity effects factors are constant and computed for the maximum admissible temperature. [18] also assumes that shield and armor resistances are constant. In reality, for lower temperatures (for example at the core of the cable where charging currents are smaller), conductivity is greater thus the skin depth decreases. In that case, the equivalent AC resistance increases. This can be explicated using Bessel equations as expressed in [16], (7) and (8), or more simply by considering the physical action of induction phenomena on the equivalent resistance.

For illustration, Fig. 4 proposes the per unit length resistance in function of the current in:

- Two 220kV AC cables with sections of respectively 500mm^2 and 1000mm^2.
- A 66kV cable, with a section of 185mm^2.
- A DC ±320kV cable, with a section of 1000mm^2.

Based on Fig. 4, we can propose some analyses, which are also a guidance for the choice of model to be used. For an AC cable, the more you increase the section the more the difference between the standards and the model proposed by H. Brakelmann is significant. This is confirmed for a smaller section of 185mm^2, where the model proposed by H. Brakelmann has a lower relative error compared to the actual resistance.

Also, for large sections the adequacy of the constant-temperature model (which is used a lot in the literature as it is given in data sheets) with the standards is more relevant. Finally, the results show that for DC cables (and any cross section), there is no difference anymore between the standards and the model proposed by H. Brakelmann.

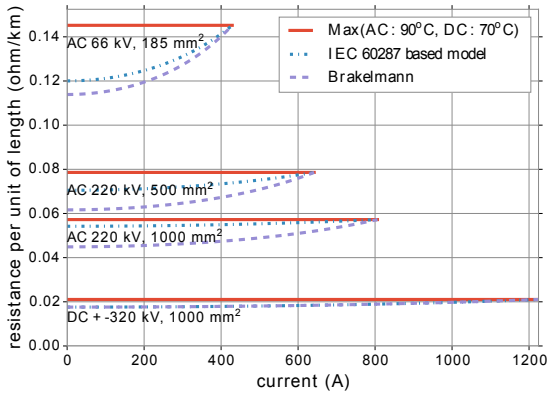

Figure. 4. Core conductor resistances depending on the current. Comparison of the models on various AC and DC cables.

B. Application of the proposed model for offshore wind power transmission

1) Simultaneous design and power management for HVAC cables

As stated by Gustavsen and Mo [13], due to distributed capacitances of HVAC cables, there is a charging current injection. As a result, the current is not uniform along the cable. Due to the distributed resistances and inductances, the voltage also evolves along the cable.

Fig. 5 and Fig. 6 propose for different distances, current and voltage distributions along the cable for a 220kV, 500mm² cross section cable instance; with compensation on both sides. The results are given for variables resistances on multiple PI section by using the exposed model based on IEC 60287.

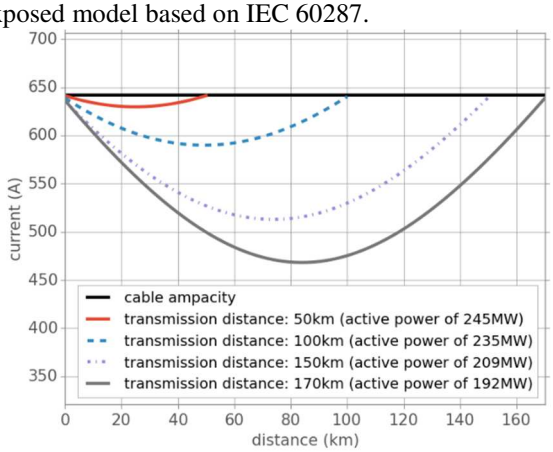

Figure. 5. Currents distribution. Example of a 220kV and 500mm² cable.

A distributed PI model of the cable is retained. It gives a sufficient accuracy if the sections are small enough. In the present work, PI sections of 1 km are used. The proposed model is integrated into a numerical load flow calculation by using the Pylon library [26] (a Python equivalent of Matpower) similarly as what is proposed in [15].

In the present work, the power management and compensation of the cable has been determined by using the following objectives and constraints: 1) Maximizing the active power to be transmitted (by imposing equality between offshore and onshore currents). 2) Minimize voltage drop along the line.

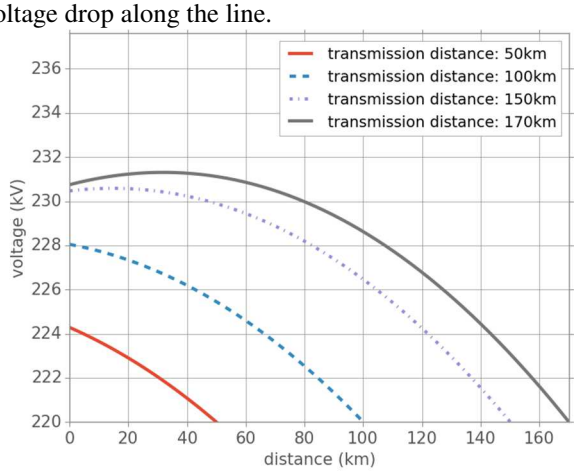

Figure. 6. Voltages distribution. Example of a 220kV and 500mm² cable.

The maximum current I_{max} transmitted by the cable comes from the ampacity model. It provides a first physical constraint to operational conditions of the cable. Another constraint is given by the maximal permanent voltage U_{max}. It is taken equal to $1.07 * U_n$ [27] (which is not an active constraint with the chosen reactive compensation configuration for 220 kV cables).

As the used strategy is to compensate the reactive power of the cable at both sides, the maximal voltage is below U_{max}. The maximal active power that can be transmitted from the wind farm shall respect the onshore and offshore current constraints, which are the critical points where both active and reactive powers are maximal. These two current boundaries lead to equations (40), (41). With $U(L)$ imposed to U_n and η is the power efficiency of the cable at maximal transmitted power.

$$P_{max}^{farm} = \sqrt{[U(0).I_{max}]^2 - Q_{offshore}^{compensation^2}} \quad (40)$$

$$P_{max}^{farm} = \frac{\sqrt{[U(L).I_{max}]^2 - Q_{onshore}^{compensation^2}}}{\eta} \quad (41)$$

Fig. 7 proposes the schematic modeling of the cable used for the computation. The PI sections are represented directly from the compensation point to the slack bus.

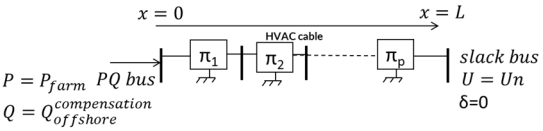

Fig. 7. Load flow case used for the determination of optimal power management for a HVAC cable for a given distance.

Fig. 9 shows the flow chart representing the practical implementation of the presented methodology. Fig. 8 shows the maximum active power transmitted obtained with the methodology for various distances and HVAC (220 kV) cables cross sections. An inflexion point can be observed in this figure, which corresponds to a distance of around 190 km. After this distance, the active power that can be transmitted collapses.

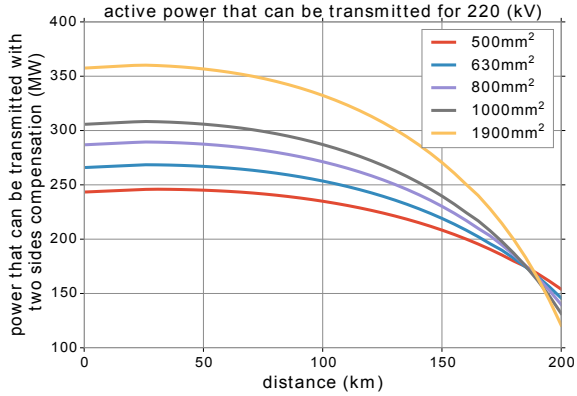

Figure. 8. Maximum active power that can be transmitted from an offshore wind farm with optimal compensation at both sides.

A typical installation consists in an offshore and onshore reactor of similar features. Reactors can be sized to fully or partially balance the cable capacitance depending on grid code requirements.

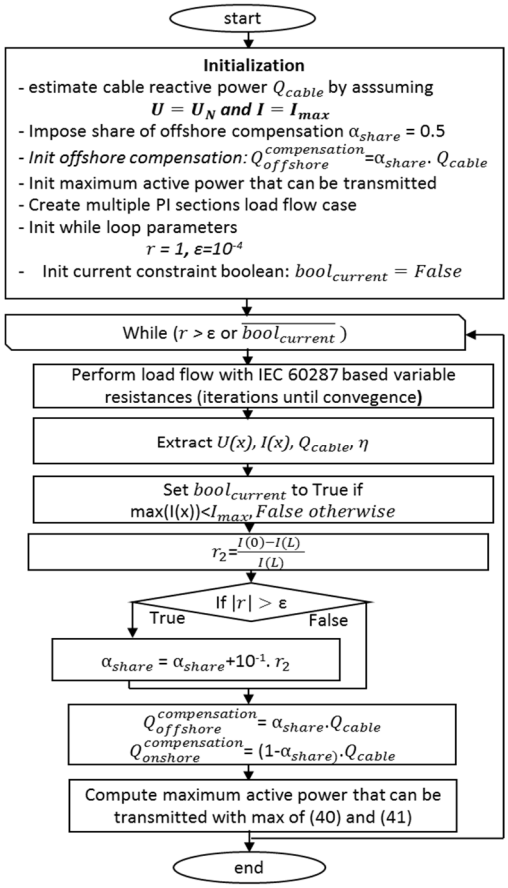

Figure. 9. Chart flow of the cable design, with reactive power compensation for a given distance and cable cross section.

In practice the compensation of long submarine cable is achieved with multiple shunt reactors. The size and location of these reactors is a tradeoff between utilization of the capacity for power transmission and the additional cost for installing several reactors [22].

2) *Economic evaluation of HVAC cable losses*

Table III proposes the annual energy losses and the life span losses costs for a discount rate of 8% over a period of 20 years of operation. The considered system is composed of a HVAC transmission cable with a 500mm2 section, 220kV, a distance of 100km and a cost of energy of 100€/MWh.

TABLE III
ANNUAL ENERGY RESULTS – 500MM^2, 220KV – 100KM

Resistance computation method	Annual energy losses (MWh)	Life span losses cost (M€)
Max temperature	30400	52
IEC standards	29300	50
H. Brakelmann	28000	48

These results show that the choice of the resistance model, i.e. one parameter of some components in the whole system, has a significant impact on levelized cost of the final infrastructure. Therefore, even in a system-driven design perspective, the good choice of model as well as its given precision are key components for pertinent tools for decision support.

VI. Conclusion

This paper has proposed cable models for the technical and economic evaluation of offshore wind generation systems based on those cables, including their optimal design and evaluation. The choice of the level of accuracy for the model at each step of this process is crucial in order to propose a relevant design and evaluation tool for decision makers.

This integrated approach is based on cables modeling. In this paper, three cables modeling are discussed; the IEC 60287 standards are fully explicated, then compared with the model proposed by H. Brakelmann and a simplification model considering a constant maximal temperature along the cable.

The comparison of the cable models is illustrated on various cables, based on their section, voltage, etc. We can see that the greater the section, the more interesting the simplification model is. Also, we checked that the model proposed by Brakelmann is correct in DC. For all other cases, the model, based on standards, is preferred.

To conclude, the proposed paper goes beyond cables modeling by describing an assessment method based on specific cables modeling, allowing including the choice of cables in a more global infrastructure assessment tool for decision support regarding optimal design of offshore wind farm grid connection.

ACKNOWLEDGMENT

This work has been carried out in the SuperGrid Institute.

REFERENCES

[1] T. Ackermann, N. B. Negra, J. Todorovic, and L. Lazaridis, “Evaluation of Electrical Transmission Concepts for Large Offshore Windfarms,” in *Copenhagen Offshore Wind Conference and Exhibition, Copenhagen*, 2005.

[2] S. Lundberg, *Wind Farm Configuration and Energy Efficiency Studies: Series DC Versus AC Layouts*. Chalmers University of Technology, 2006.

[3] J. S. González, M. B. Payán, and J. R. Santos, “Optimum design of transmissions systems for offshore wind farms including decision making under risk,” *Renewable energy*, vol. 59, pp. 115–127, 2013.

[4] K. Nieradzinska, C. MacIver, S. Gill, G. Agnew, O. Anaya-Lara, and K. Bell, “Optioneering analysis for connecting Dogger Bank offshore wind farms to the GB electricity network,” *Renewable Energy*, vol. 91, pp. 120–129, 2016.

[5] G. Stamatiou, K. Srivastava, M. Reza, and P. Zanchetta, “Economics of DC wind collection grid as affected by cost of key components,” in *World Renewable Energy Congress*, 2011, vol. 159, p. 164.

[6] M. Banzo and A. Ramos, “Stochastic optimization model for electric power system planning of offshore wind farms,” *IEEE Transactions on Power Systems*, vol. 26, no. 3, pp. 1338–1348, 2011.

[7] H. Ergun, D. Van Hertem, and R. Belmans, “Transmission System Topology Optimization for Large-Scale Offshore Wind Integration,” *Sustainable Energy, IEEE Transactions on*, vol. 3, no. 4, pp. 908–917, Oct. 2012.

[8] S. Rodrigues, C. Restrepo, G. Katsouris, R. Teixeira Pinto, M. Soleimanzadeh, P. Bosman, and P. Bauer, “A Multi-Objective Optimization Framework for Offshore Wind Farm Layouts and Electric Infrastructures,” *Energies*, vol. 9, no. 3, p. 216, 2016.

[9] M. D. P. Gil, J. Domınguez-Garcıa, F. Dıaz-González, M. Aragüés-Peñalba, and O. Gomis-Bellmunt, “Feasibility analysis of offshore wind power plants with DC collection grid,” *Renewable Energy*, vol. 78, pp. 467–477, 2015.

[10] P. MONJEAN, “Optimisation de l’architecture et des flux énergétiques de centrales à énergies renouvelables offshore et onshore équipées de liaisons en continu,” PhD thesis, Arts et Métiers ParisTech, 2012.

[11] M. de Prada Gil, O. Gomis-Bellmunt, and A. Sumper, “Technical and economic assessment of offshore wind power plants based on variable frequency operation of clusters with a single power converter,” *Applied Energy*, vol. 125, pp. 218–229, 2014.

[12] W. Fischer, R. Braun, and I. Erlich, “Low frequency high voltage offshore grid for transmission of renewable power,” in *Innovative Smart Grid Technologies (ISGT Europe), 2012 3rd IEEE PES International Conference and Exhibition on*, 2012, pp. 1–6.

[13] B. Gustavsen and O. Mo, “Variable Transmission Voltage for Loss Minimization in Long Offshore Wind Farm AC Export Cables,” *IEEE Transactions on Power Delivery*, vol. 32, no. 3, pp. 1422–1431, Jun. 2017.

[14] A. Madariaga, J. L. Martı, I. Zamora, S. Ceballos, O. Anaya-Lara, and others, “Effective Assessment of Electric Power Losses in Three-Core XLPE Cables,” *IEEE Transactions on Power Systems*, vol. 28, no. 4, pp. 4488–4495, 2013.

[15] X. Yuan, H. Fleischer, G. Sande, and L. Solheim, “Integration of IEC 60287 in Power System Load Flow for Variable Frequency and Long Cable Applications,” 2013.

[16] *60287-1: Electric cables – Calculation of the current rating - Current rating equations (100 % load factor) and calculation of losses*. IEC.

[17] *60287-2: Electric cables – Calculation of the current rating, Thermal resistance – Calculation of thermal resistance*. IEC.

[18] H. Brakelmann, “Loss determination for long three-phase high-voltage submarine cables,” *European transactions on electrical power*, vol. 13, no. 3, pp. 193–197, 2003.

[19] *XLPE Submarine Cable Systems Attachment to XLPE Land Cable Systems User´s Guide*. ABB.

[20] O. Dahmani, “Modélisation, optimisation et analyse de fiabilité de topologies électriques AC des parcs éoliens offshore,” PhD thesis, STIM, 2014.

[21] A. Papadopoulos, "Modeling of collection and transmission losses of offshore wind farms for optimization purposes," Master thesis, Delft University of Technology, 2015.
[22] *60228: Conductors of insulated cables*. IEC.
[23] Nexans, *Submarine Power Cables*. .
[24] M. M. Hatlo and J. J. Bremnes, "Current dependent armor loss in three-core cables: comparison of FEA results and measurements," *GIGRE*, 2014.
[25] J. Pilgrim, S. Catmull, R. Chippendale, and P. Lewin, "Offshore Wind Farm Export Cable Current Rating Optimisation," in *EWEA*, 2013.
[26] R. Lincoln, "Pylon library, Copyright (C) 1996-2010 Power System Engineering Research Center (PSERC)."
[27] L. Colla, F. M. Gatta, A. Geri, S. Lauria, and M. Maccioni, "Steady-state operation of very long EHV AC cable lines," *PowerTech, 2009 IEEE Bucharest*, 2009.

Swann Gasnier was born in France, in 1990, he received the M.Sc. degree from Ecole Centrale Lyon, France, in 2014. He received the Ph.D. degree in electrical engineering from Centrale Lille, France, in 2017. His PhD research was conducted in SuperGrid Institute, in partnership with L2EP laboratory. Since then, he works as a data scientist consultant. His main fields of interest are operational research, statistics and computer science, with an emphasis to the energy field.

Aymeric Andre was born in France, in 1989. He studied Electrical Power Engineering at the Norwegian University of Science and Technology of Trondheim. He received his MSc degree in 2015 from the department of electrical engineering of Ecole Supérieur de Chimie Physique Electronique de Lyon. In 2015 he took a position as researcher at the Nexans Research Center of Lyon where he leads a research program on meshed subsea networks for the SuperGrid Institute. His research interests include subsea cable system technologies, HVAC and HVDC transmissions for offshore wind.

Vincent Debusschere was born in France, in 1981. He joined the Ecole Normale Superieure de Cachan (ENS Cachan), France, in 2001, for studies in the field of applied physics. He received a Masters degree in information, systèmes et technologie (IST) from University Paris-Sud XI and ENS Cachan, Saclay, France, in 2005, and the Ph.D. degree in ecodesign of electrical machines from ENS Cachan, in 2009. He joined the Grenoble Electrical Engineering Laboratory (G2Elab) from the Grenoble Institute of Technology, France, in 2010 as an Associate Professor. His research interests include renewable energy integration, energy efficiency, flexibility levers for Smart grids, economic and environmental criteria for optimization and design of power systems.

Serge Poullain has been working with Supergrid Institute since 2014, as Sub-program Manager. He received his MSc degree in Robotics and Electro-mechanical Engineering and his Ph.D. degree in Systems Control both from the Université de Technologie de Compiègne (UTC), France, in 1986 and 1991 respectively. In 2009, he received the Accreditation to Supervise Research (HDR) from the University of Orsay, France. In past years, he worked in the field of modelling and automatic control for both industrial AC drives and FACTS devices embedded in AC grid systems. He also had some interests in risk analysis of large power systems. Currently, his interests include HVDC systems focusing on architecture principles studies and optimization considering both technical and economic aspects.

Bruno Francois (M'96–SM'06) was born in 1969. He received the Ph.D. degree in electrical engineering from the University of Science and Technology of Lille (USTL), France, in 1996. He is with the Laboratory of Electrical Engineering and Power Electronics of Lille (L2EP), Lille, France, and is a Professor with the Department of Electrical Engineering of Ecole Centrale de Lille, Cité Scientifique, Villeneuve d'Ascq Cedex, France. His research interests include advanced energy management Systems and automation of power systems, architectures of future electrical networks, uncertainty and probability for optimization of electrical systems

Philippe Egrot received the Engineering degree from the National Polytechnic Institute of Grenoble (INPG), Grenoble, France.
He began his career at the Telecommunications Department, MATRA Telecom, in 1986. After joining Electricité Réseau Distribution France, the French Distribution System Operator, in 1989, he took the opportunity to reach the Électricité de France Research and Development Division, as a mechanical engineer to work on tests and modeling on overhead line equipment and lattice towers. Following this, he managed several laboratories, including the High Voltage and Mechanics Climatic Laboratory in 2000 and the High Power Laboratory in 2003.
Mr. Egrot was involved in several CIGRE and IEC Technical Committees and was a member of ASEFA, the French certification body.